Supporting Information

A Universal Descriptor Based on p_z-Orbital for The Catalytic Activity of Multi-doped Carbon Bifunctional Catalysts for Oxygen Reduction and Evolution

Jiameng Ma[1], Qiuming Zhi[1], Lele Gong[1], Yang Shen[1], Defeng Sun[1], Yongjian Guo[1], Lipeng Zhang[1*], Zhenhai Xia[2*]

Calculation Details

In acidic environment, OER could occur over N-doped graphene in the following four electron reaction paths,

$$H_2O(l) + * \rightarrow OH^* + (H^+ + e^-) \quad \text{(S1)}$$

$$OH^* \rightarrow O^* + (H^+ + e^-) \quad \text{(S2)}$$

$$O^* + H_2O(l) \rightarrow OOH^* + (H^+ + e^-) \quad \text{(S3)}$$

$$OOH^* \rightarrow * + O_2(g) + (H^+ + e^-) \quad \text{(S4)}$$

where * stands for an active site on the graphene surface, (l) and (g) refer to liquid and gas phases respectively, and O*, OH* and OOH* are adsorbed intermediates. The ORR can proceed incompletely through a two-step two-electron pathway that reduces O_2 to hydrogen peroxide, H_2O_2, or completely via a direct four-electron process in which O_2 is directly reduced to water, H_2O, without involvement of hydrogen peroxide. Here we study the complete reduction path because the previous and current results showed that the ORR proceeds on graphene-based materials through the four-electron transfer mechanism.[1] The ORR mechanism is summarized using the following elementary

steps.

$$O_2^* + (H^+ + e^-) \rightarrow OOH^* \quad \text{(S5)}$$

$$OOH^* + (H^+ + e^-) \rightarrow O^* + H_2O(l) \quad \text{(S6)}$$

$$O^* + (H^+ + e^-) \rightarrow OH^* \quad \text{(S7)}$$

$$OH^* + (H^+ + e^-) \rightarrow * + H_2O(l) \quad \text{(S8)}$$

where * stands for an active site on the compounds, (l) and (g) refer to liquid and gas phases respectively, and O*, OH* and OOH* are adsorbed intermediates, which are bonding with on carbon atom with –C-O- form.

The overpotentials of ORR and OER processes can be determined by examining the reaction free energies of the different elementary steps, and the rate-limiting steps were determined by selecting the maximum overpotentials among the elementary reactions. The thermochemistry of these electrochemical reactions was obtained by using density functional theory (DFT) calculations in conjunction with SHE model developed by Norskov and co-workers.[2,3]

The absorption energies of O*, OH* and OOH* were calculated as follows,[3]

$$\Delta E_{OH*} = E(OH*) - E(*) - (E_{H_2O} - \frac{1}{2}E_{H_2}) \quad \text{(S9)}$$

$$\Delta E_{OOH*} = E(OOH*) - E(*) - (2E_{H_2O} - \frac{3}{2}E_{H_2}) \quad \text{(S10)}$$

$$\Delta E_{O*} = E(O*) - E(*) - (E_{H_2O} - E_{H_2}) \quad \text{(S11)}$$

in which E(*), E(OH*), E(O*) and E(OOH*) denote to the energies of a clean surface and surfaces adsorbed with OH*, O* and OOH* respectively. E_{H_2O} and E_{H_2} are the energies of H_2O and H_2 molecules in the gas phase calculated DFT method.

The reaction free energy ΔG of each step is defined as the difference between free energies of the initial and final states:[4]

$$\Delta G = \Delta E + \Delta ZPE - T\Delta S + \Delta G_U + \Delta G_{pH} \quad \text{(S12)}$$

where ΔE is the reaction energy of reactant and product molecules adsorbed on catalyst surface, obtained from DFT calculations, T is the temperature and ΔS is entropy change, ZPE represents for the zero-point energy, $\Delta G_U = -eU$, where U is the potential applied at

the electrode, and e is the transferred charge, $^{\Delta G_{pH}}$ is the correction of the H^+ free energy defined as:

$$\Delta G_{pH} = -k_B T ln[H^+] \quad \text{(S13)}$$

The overpotentials of OER and ORR can be calculated by the method which developed by Norskov et al. as following.[3]

$$G_{OER} = max\{\Delta G_1, \Delta G_2, \Delta G_3, \Delta G_4\} \quad \text{(S14)}$$

$$\eta_{OER} = \frac{G_{OER}}{e} - 1.23V \quad \text{(S15)}$$

$$G_{ORR} = max\{\Delta G_5, \Delta G_6, \Delta G_7, \Delta G_8\} \quad \text{(S16)}$$

$$\eta_{ORR} = \frac{G_{ORR}}{e} + 1.23V \quad \text{(S17)}$$

Where $^{\Delta G_1, \Delta G_2, \Delta G_3, \Delta G_4, \Delta G_5, \Delta G_6, \Delta G_7, \Delta G_8}$ are the free energy of reactions (S1)-(S8).

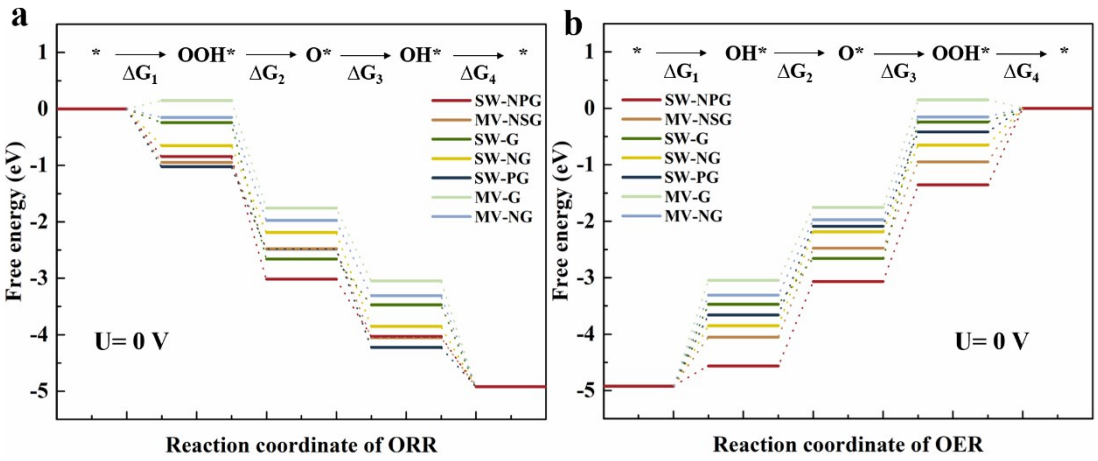

Figure S1. Free energy diagrams and reaction pathways (U = 0 V) for (a) ORR and (b) OER proceeding at the best active site on defective graphene structures.

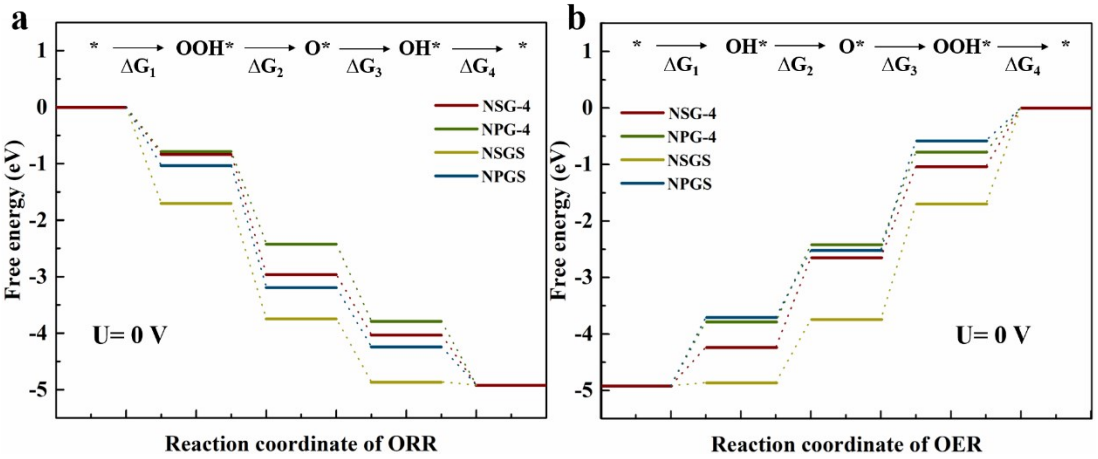

Figure S2. Free energy diagrams and reaction pathways (U = 0 V) for (a) ORR and (b) OER proceeding at the best active site on the defective graphene clusters and defective graphene structures.

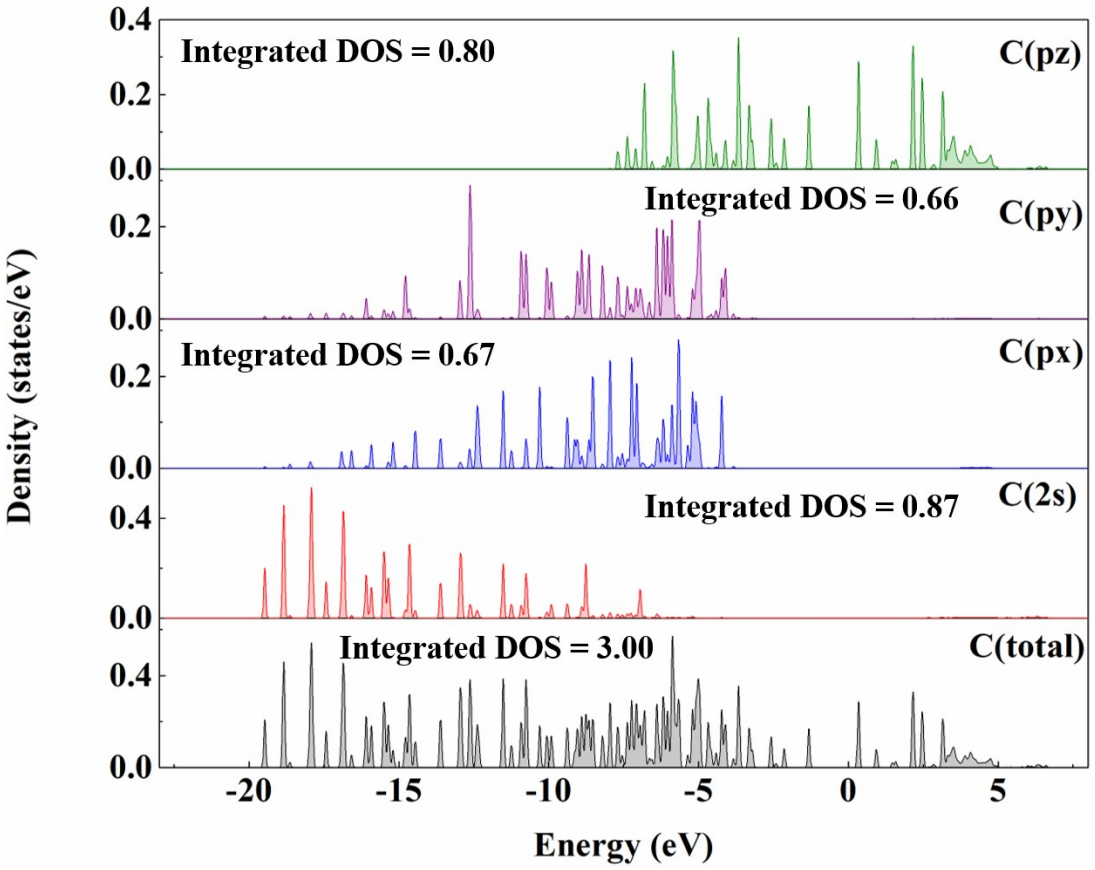

Figure S3. Total density of states of C atom on graphene and projected density of states for 2*s*, p_x, p_y and p_z orbital of C atom.

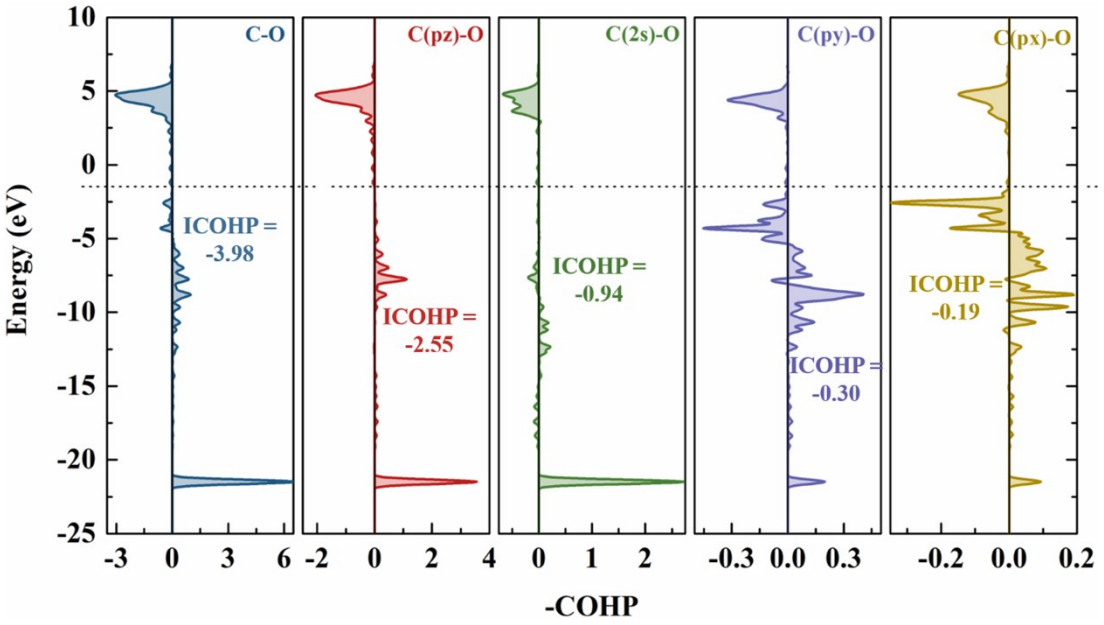

Figure S4. COHP analyses of C-O, C(p_z)-O, C(2s)-O, C(p_y)-O and C(p_x)-O bonding interactions of OH* adsorbed on edged C and their corresponding ICOHP values. The dotted line represents Fermi level.

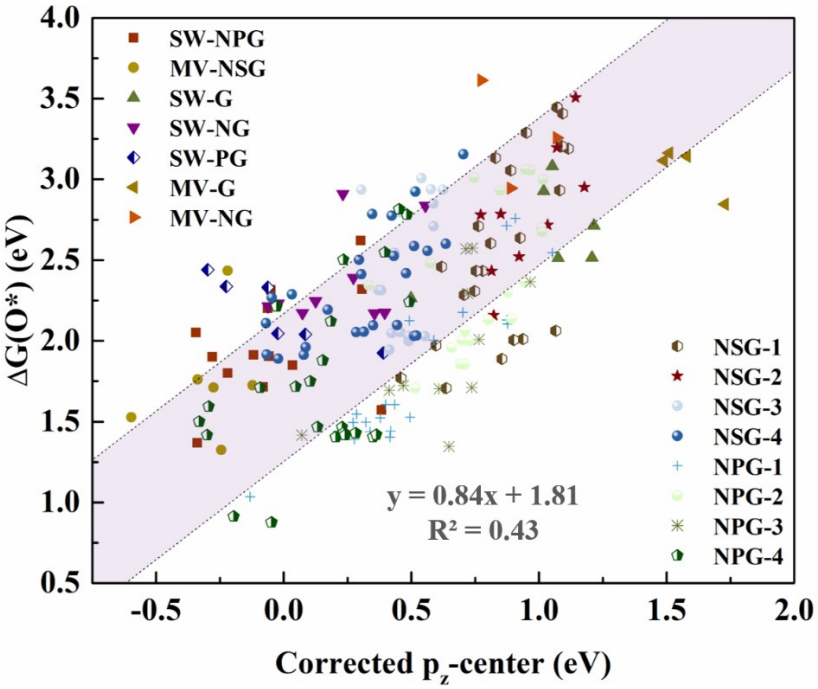

Figure S5. Correlation of ΔG(O*) and p_z-center after corrected by the amended value for edged C.

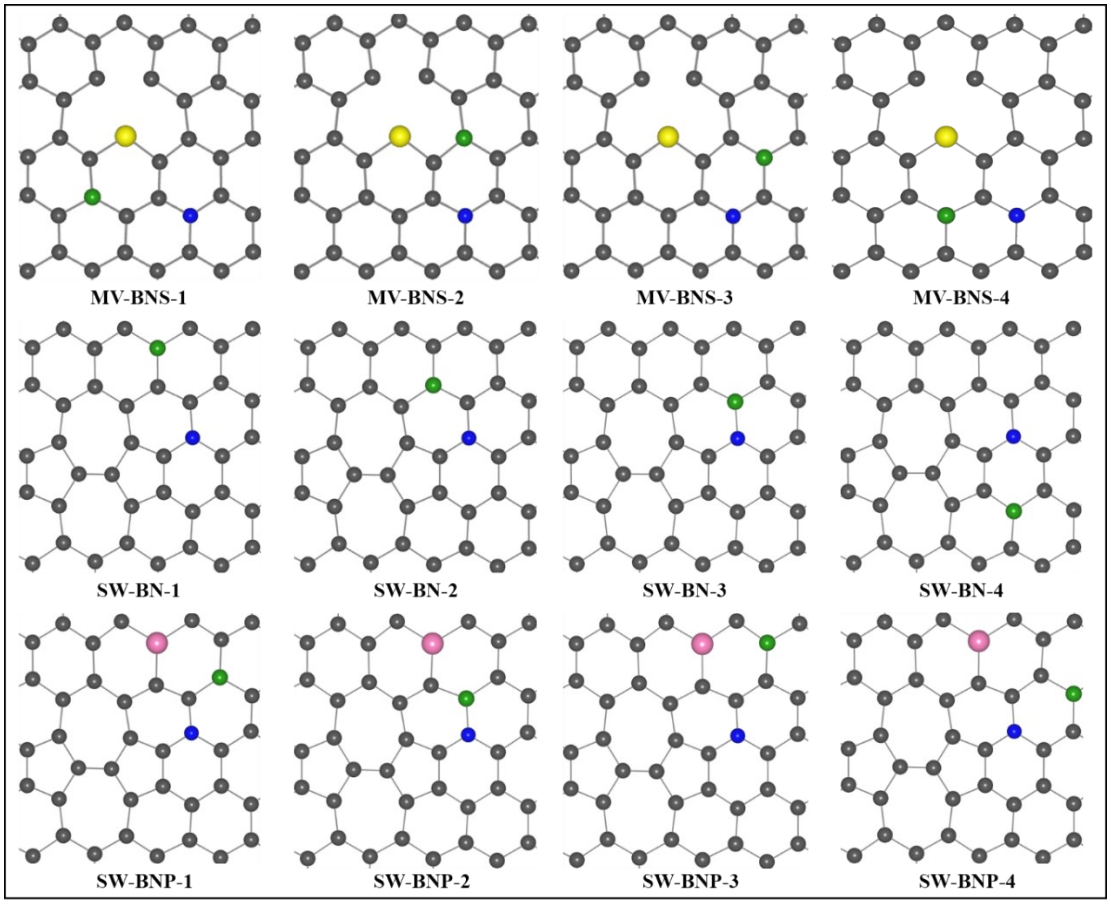

Figure S6. Configurations of various graphene structures codoped with heteroatoms and structural defects. The black, blue, green, yellow and pink atoms denote carbon, nitrogen, boron, sulfur and phosphorus elements, respectively.

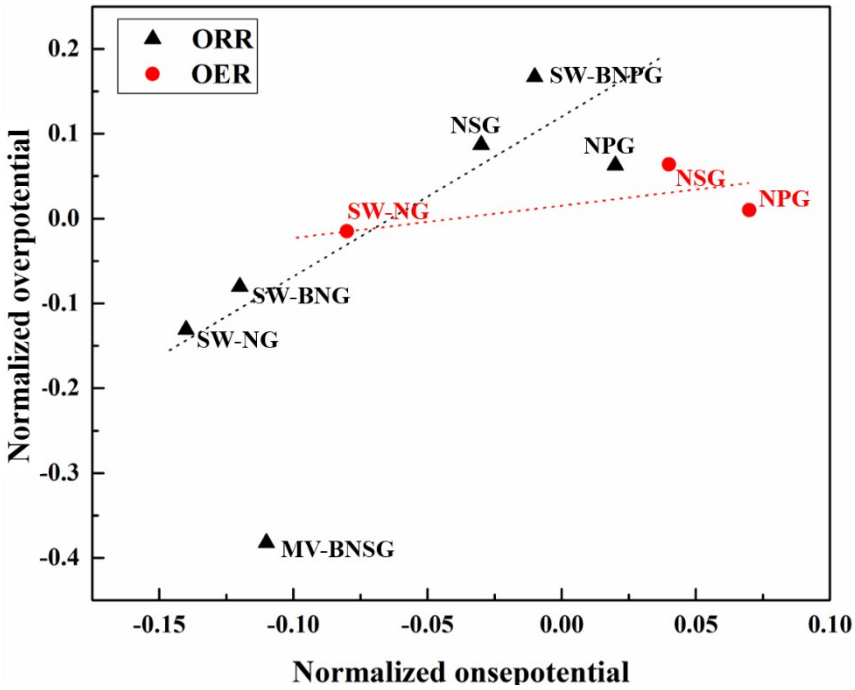

Figure S7. Correlation between the normalized onset potential in experimental works and the normalized DFT overpotential in this work. For ORR, the experimental onset potentials of NSG[5], NPG[6], SW-BNPG[7], SW-BNG[8], SW-NG[9], MV-BNSG[10] were normalized by subtracting onset potential of Pt/C in the same experiment. For OER, the experimental onset potentials of NSG[11], NPG[6] and SW-NG[9] were normalized by subtracting onset potential of RuO_2 in the same experiment. The values of DFT overpotential of Pt/C (ORR) or RuO_2 (OER) minus DFT overpotentials of these structures in this work are used as the vertical coordinates.

Table S1. Major descriptors identified for the electrocatalytic properties of different materials.

Descriptor	Calculation	Reaction	Material system
d-band center[12]	$\frac{\int_{-\infty}^{0} \rho_d E dE}{\int_{-\infty}^{0} \rho_d dE}$	ORR	Transition metals and transition metal alloys
$\Delta G(OH^*)$[13]	G(OH*)-G(*)-G(OH)	ORR and OER	N-doped graphene
Φ[14]	$\frac{E_X}{E_C} \times \frac{A_X}{A_C}$	ORR, OER and IRR	Heteroatoms-doped graphene and CNTS
O_{p_z}[15]	$[\int_{-\infty}^{0} \rho_{p_z} dE]_{active\ site} - [\int_{-\infty}^{0} \rho_{p_z} dE]$	ORR	N,B doped graphene
$D_{p_z}(E_F)$[15]	The values of p_z projected density of state at the Fermi level	ORR	N,B doped graphene
E_p[16]	Position of the highest peak of the active site's DOS	HER	Doped graphene
Φ[17]	$\frac{V_M \times E_M}{r_M}$	CO_2RR	Single-atom catalysts

Table S2. p_z-center values of graphitic-C and edge-C with almost the same adsorption energy of OH*

edge-C	graphitic-C	difference of pz-center	difference of ΔG(OH*)
-1.338	-2.244	0.906	0.002
-1.503	-2.185	0.682	0.002
-1.825	-2.410	0.584	0.001
-1.708	-2.243	0.534	0.002
-2.171	-2.793	0.622	-0.010
-1.783	-2.349	0.566	-0.015
-1.573	-2.307	0.733	-0.004
-1.593	-2.627	1.034	0.010
-1.413	-1.950	0.537	-0.002
-1.552	-2.104	0.552	0.007
-1.685	-2.226	0.541	-0.010
-1.807	-2.745	0.938	-0.015
-1.844	-2.322	0.478	0.007

Reference

1. L. Zhang and Z. Xia, *J. Phys. Chem. C*, 2011, **115**, 11170-11176.

2. J. K. Nørskov, J. Rossmeisl, A. Logadottir, L. Lindqvist, J. R. Kitchin, T. Bligaard and H. Jónsson, *J. Phys. Chem. B*, 2004, **108**, 17886-17892.

3. I. C. Man, H. Y. Su, F. Calle-Vallejo, H. A. Hansen, J. I. Martínez, N. G. Inoglu, J. Kitchin, T. F. Jaramillo, J. K. Nørskov and J. Rossmeisl, *ChemCatChem*, 2011, **3**, 1159-1165.

4. S. Zuluaga and S. Stolbov, *J. Chem. Phys.*, 2011, **135**, 134702.

5. J. Liang, Y. Jiao, M. Jaroniec and S. Z. Qiao, *Angew. Chem. Int. Ed. Engl.*, 2012, **51**, 11496-11500.

6. R. Li, Z. D. Wei, and X. L. Gou, *ACS Catal.*, 2015, **5**, 4133-4142.

7. P. Routh, S.-H. Shin, S.-M. Jung, H.-J. Choi, I.-Y. Jeon and J.-B. Baek, *Eur. Polym. J.*, 2018, **99**, 511-517.

8. Y. Zheng, Y. Jiao, L. Ge, M. Jaroniec and S. Z. Qiao, *Angew. Chem. Int. Ed. Engl.*, 2013, **52**, 3110-3116.

9. Y. Jia, L. Zhang, A. Du, G. Gao, J. Chen, X. Yan, C. L. Brown and X. Yao, *Adv. Mater.*, 2016, **28**, 9532-9538.

10. S. B. Ingavale, I. M. Patil, H. B. Parse, N. Ramgir, B. Kakade and A. Swami, *New J. Chem.*, 2018, **42**, 12908-12917.

11. J. J. Zhao, Y. M. Liu, X. Quan, S. Chen, H. M. Zhao and H. T. Yu, *Electrochim. Acta*, 2016, **204**, 169-175.

12. C. Tsai, K. Chan, J. K. Nørskov and F. Abild-Pedersen, *J. Phys. Chem. Lett.*,

2014, **5**, 3884-3889.

13. M. Li, L. Zhang, Q. Xu, J. Niu and Z. Xia, *J. Catal.*, 2014, **314**, 66-72.

14. Z. Zhao, M. Li, L. Zhang, L. Dai and Z. Xia, *Adv. Mater.*, 2015, **27**, 6834-6840.

15. S. Sinthika, U. V. Waghmare and R. Thapa, *Small*, 2018, **14**, 1703609.

16. Y. Jiao, Y. Zheng, K. Davey and S.-Z. Qiao, *Nat. Energy*, 2016, **1**, 16130.

17. L. Gong, D. Zhang, C. Y. Lin, Y. Zhu, Y. Shen, J. Zhang, X. Han, L. Zhang and Z. Xia, *Adv. Energy Mater.*, 2019, **9**, 1902625.